

JGR Space Physics

RESEARCH ARTICLE

10.1029/2019JA026829

Key Points:

- The growth phase auroral arc was associated with the enhanced *E* layer electron density corresponding to about 13-MHz plasma frequency
- Enhanced *E* layer ionization caused bending and ground scatter of the 36.9-MHz radio waves transmitted at low elevation
- Amplitude of the radar ground scatter was modulated at a frequency of a few hertz, and such modulation was found in auroral luminosity

Supporting Information:

- Supporting Information S1
- Data Set S1
- Data Set S2
- Movie S1

Correspondence to:

A. Kozlovsky,
alexander.kozlovsky@oulu.fi

Citation:







Kozlovsky, A., Shalimov, S., Oyama, S., Hosokawa, K., Lester, M., Ogawa, Y., & Hall, C. (2019). Ground echoes observed by the meteor radar and high-speed auroral observations in the substorm growth phase. *Journal of Geophysical Research: Space Physics*, 124, 9278–9292. <https://doi.org/10.1029/2019JA026829>

Received 11 APR 2019

Accepted 10 AUG 2019

Published online 8 NOV 2019

Ground Echoes Observed by the Meteor Radar and High-Speed Auroral Observations in the Substorm Growth Phase

A. Kozlovsky¹ , S. Shalimov^{2,3}, S. Oyama^{4,5,6} , K. Hosokawa^{5,7} , M. Lester⁸ , Y. Ogawa⁶ , and C. Hall⁹ 

¹Sodankylä Geophysical Observatory, University of Oulu, Sodankylä, Finland, ²Institute of Physics of the Earth, Moscow, Russia, ³Space Research Institute, Moscow, Russia, ⁴Institute for Space-Earth Environmental Research, Nagoya University, Nagoya, Japan, ⁵Ionospheric Physics Unit, University of Oulu, Oulu, Finland, ⁶National Institute of Polar Research, Tokyo, Japan, ⁷Department of Communication Engineering and Informatics, University of Electro-Communications, Tokyo, Japan, ⁸Department of Physics and Astronomy, University of Leicester, Leicester, UK, ⁹Tromsø Geophysical Observatory, The Arctic University of Norway, Tromsø, Norway

Abstract Multi-instrument observations by a meteor radar (MR), auroral cameras, ionosondes, and ground magnetometers were made in Northern Europe at auroral latitudes (between 64° and 72° corrected geomagnetic latitude) at 22–24 magnetic local time in the substorm growth phase. The southward drifting growth phase auroral arc was associated with enhanced electron density up to $2 \cdot 10^{12} \text{ m}^{-3}$ (corresponding to a plasma frequency, *foEs* of about 13 MHz) at about 110-km altitude. Such an enhanced *E* layer electron density caused bending toward the ground of the MR radio waves transmitted at a frequency, *f_r*, of 36.9 MHz and at low elevation (*el.* < 25°), such that the radar received ground echoes characterized by a near-zero Doppler shift. The amplitude of the echoes was modulated at a frequency of a few hertz, and a similar modulation was found in the auroral luminosity at 427.8 nm near the location of the bending of MR radio waves. The modulation was due to irregular (random) fluctuations of auroral precipitation. Although such a few-hertz variation of the auroral precipitation cannot produce more than 1% modulation of the ionospheric electron density, even such a small modulation can lead to 50% modulation of the MR ground scatter provided *foEs* $\approx f_r \sin(el.)$. The ionosonde and MR data provide evidence that this condition was satisfied in the present case. Due to a high-frequency (>2 Hz) amplitude modulation of the ground scatter, the MR erroneously accepts such signals as echoes from meteor trails.

Plain Language Summary It is known that due to the ionospheric recombination time of the order of tens of seconds, fast few-hertz variations of auroral precipitation cannot produce noticeable enough variations in the ionospheric plasma density to be detected by radars. Nevertheless, such high-frequency variations were detected in the ground scatter of the meteor radar operated at a frequency of 37 MHz. It was possible due to the enhanced ionospheric electron density at about 110 km altitude associated with the auroral arc in the substorm growth phase. We have shown that if the electron density exceeds some critical value, the radar waves can be bended toward the ground, reflected from the ground and returned to the radar. Otherwise, the radio waves pass through the ionosphere and never come back. Thus, even small changes of the *E* layer electron density (less than 1%) may cause noticeable modulation of the radar return. This makes possible radar monitoring of the fast variations of auroral precipitation.

1. Introduction

This paper is a continuation of the study of Kozlovsky and Lester (2015) where some peculiarities of the meteor radar (MR) observations at auroral latitudes in Northern Europe were first reported. The MR used in the study is an all-sky interferometric MR (SKiYMET), which is designed for detecting ionized meteor trails at heights above 70 km. For the detected trails, their position, Doppler velocity of the scatter from these trails, and the decay time of the scatter from the trails are determined. Then, the Doppler velocity is used to estimate the atmospheric winds at these heights, while the decay time is used to estimate the mesospheric temperature (Hocking et al., 2001).

An important part of the MR processing software is the analysis of the returned signals to select only those signals that are believed to be echoes from meteor trails. The characteristic features used to distinguish meteor echoes from other signals include their rapid onset, relatively short duration (typically less than 2 s), and quasi-exponential decay. The great majority of the MR detections are indeed echoes from meteor trails, but Kozlovsky and Lester (2015) noticed that in some rare cases, the MR operating at auroral latitudes may erroneously accept certain nonmeteor echoes in the region of the midnight aurora as echoes from meteor trails. The amplitude of such nonmeteor echoes exhibits quasiperiodic or irregular oscillations at a frequency of about 2 Hz or higher, such that individual amplitude peaks resemble meteor echoes. However, the autocorrelation function of such signals is typically much broader than that of meteor echoes. As the decay time of trails, that is, the half-life time, τ , is calculated from the width of the autocorrelation function, the system often cannot determine the decay time of these nonmeteor echoes, which is indicated as a missing τ value in the meteor parameter data file. Such detections were named auroral nonexponentially decayed (NED) echoes. They appear as rare events (on average, about 15 events per a year) lasting from 10 min to about 2 hr, during which a few tens to a few hundreds of NED echoes are observed (Kozlovsky & Lester, 2015).

The auroral NED echoes are detected at low elevation on the northern horizon and constantly have near-zero Doppler shift, such that Kozlovsky and Lester (2015) concluded that the echoes are ground backscatter from either the ground or the sea. This is similar to Super Dual Auroral Radar Network detection of signatures of the gravity waves, which quasiperiodically affect ionospheric refraction of the radar waves and therefore change the power of the ground scatter return (Samson et al., 1989, 1990). However, the period of variation and the nature of the modulation in the cases of NED and gravity waves are entirely different. Finally, Kozlovsky and Lester (2015) suggested that “auroral NED echoes are ground backscatters of the MR waves refracted in the ionosphere and passed through the region, where pulsating aurora (at a frequency higher than 1.7 Hz) occurs and causes quasi-periodical modulation of the wave propagation conditions, which leads to corresponding modulation of the power of ground backscatter return.”

The hypothesis of pulsating aurora needed confirmation by simultaneous observations with a high-speed auroral camera, but permanent auroral observation in the region was routinely made at a rate of one frame in a few seconds at best, which is not enough to resolve the 2-Hz variations. Only at the end of 2016 suitable high-speed cameras were installed in Northern Europe in association with the Exploration of energization and Radiation in Geospace project (Miyoshi et al., 2018). In the present paper we study in detail a unique case from 6 November 2016 when the MR detected NED auroral echoes from the region where successful auroral observations were made with the high-speed camera.

Thus, the scientific aim of the paper is to check the hypothesis of the VHF (30–40 MHz) radar ground scatter modulated by auroral precipitation. First, we describe the MR data obtained during the event. Second, on the basis of the ionospheric sounding data, we determine height and location of the MR targets and make comparison with the auroral optical data. Finally, we suggest a suitable interpretation of the observations and discuss the observations in association with the background geophysical conditions.

2. Instruments and Data

The Sodankylä Geophysical Observatory (SGO, geographic coordinates 67°22'N, 26°38'E) is located at the corrected geomagnetic (CGM) latitude of 64°, which is statistically in the vicinity of the equatorward edge of the nightside auroral oval. The SKiYMET MR at SGO operates at a frequency of 36.9 MHz, with a transmitted power of 15 kW. The transmitter antenna has a broad radiation pattern designed to illuminate a large expanse of the sky. The receiving antenna array is arranged as an interferometer and phase differences in the signals arriving at each of the five antennas are used to determine the direction of arrival (both azimuth and elevation angles). In most cases the direction is determined unambiguously, although angle errors may occur sometime when several targets are detected simultaneously at the same gate. The pulse repetition frequency of MR transmissions is 2,144 KHz, which leads to the 70-km range ambiguity. To reduce the range ambiguity, the MR data analysis algorithm assumes that meteor trails are at heights between 70 and 110 km. This assumption, however, is not applicable to ground scatter, so that the range data are not utilized in the present study.

To monitor the aurora colocated with the NED echoes, we use the high-speed all-sky camera (ASC) installed in Tromsø. The geographic coordinates of the camera are 69°35'N, 19°14'E. This camera observed aurora at the wavelength of 427.8 nm (blue emission) making 10 frames per second. Due to the short lifetime of the blue emission (10^{-7} s), it is suitable to observe few-hertz auroral pulsations (fluctuations). The spatial resolution of the ASC varies from 0.2 km near zenith to 10 km at an elevation of 20°. The height of the blue emission is typically of the order of 100 km, so that the ASC allows auroral observations in the surrounding area within about 250 km.

For auroral observations over a larger area we use red emission (630 nm) data of the ASC installed in Abisko (68.36°N, 18.82°E), the latitude of which is between Tromsø and SGO. Due to the red emission height of about 200 km, it makes possible monitoring aurorae at the distance up to 500 km, although temporal resolution of these observations is poor because of the long lifetime (110 s) of the red emission.

Ionospheric electron density data were obtained from the Digisonde of the Tromsø Geophysical Observatory, which is at about the same location as the Tromsø ASC. This is a standard Lowell Digisonde (<http://www.digisonde.com>) making vertical ionospheric sounding once in 15 min (Hall & Hansen, 2003). Additionally, data from the SGO ionosonde, a frequency-modulated continuous wave chirp sounder developed at SGO (Enell et al., 2016), were used. Sounding is made once a minute, and each sweep lasts for 30 s, during which the transmitted signal frequency is linearly increased from 0.5 to 16 MHz. Due to its dynamic range of 90 dB, the SGO ionograms allow studies of ionospheric structures at high resolution.

To monitor geophysical conditions in the surrounding area, data from the IMAGE magnetometer network (Tanskanen, 2009) were used. In the region of the observations, the magnetic local time is about UT + 3 hr.

3. MR Observations

Parameters of the MR echoes detected between 12 and 24 UT on 6 November 2016 are presented in Figure 1 where elevation, azimuth, and Doppler line-of sight velocity (+ away) are shown in Panels a, b, and c, respectively. The red dots indicate NED echoes as determined by the lack of a delay time, τ , in the MR data products. The auroral NED echoes were observed between 19 and 21 UT predominantly at low elevation below 25° at the azimuth slowly changing from north to west. The Doppler velocity of these echoes was a few meters per second, which in the case of ground scatter indicates slow vertical motion of the ionospheric plasma. This is a typical event illustrating auroral NED echoes as was specified in Kozlovsky and Lester (2015).

In routine MR operation for each echo accepted as a meteor, a short 4-s record of the signals (real and imaginary components) received at five antennas is archived. An example of such a record for a NED echo detected at 19:40:13 UT is shown in Figure 2, where the amplitude of the signal received at one of the antennas is presented versus time (zero time corresponds to the time of “meteor” detection). The amplitude exhibits quasiperiodic oscillations at a frequency about 2 Hz. Altogether, 249 NED echoes were detected during this event. Their amplitude records are presented in Figure 3a as a color-coded plot as a function of the record duration time (horizontal axis) and time of detection (vertical axis). This plot shows that more or less periodic signals of large amplitude were detected between 1928 and 1942 UT, whereas at other times the amplitude variations were rather irregular. Figure 3b on the right presents the corresponding Doppler spectra, which show a near-zero velocity for all the NED echoes.

To compare the NED echoes with auroral observations, one needs to locate the place in the ionosphere where the radio wave path was refracted or/and reflected (bent) toward the ground. This requires some knowledge or reasonable assumption of the height at which the bending occurs. Therefore, in the next section we consider the ionospheric conditions during the event.

4. Ionospheric Ionization

Black dots in Figure 4a show the azimuth of the NED MR echoes during 18–22 UT (the same as the red dots in Figure 1b). The horizontal dashed red line indicates the direction from SGO toward the Tromsø ASC, which is at -44° from north (negative azimuth means an angle from north to west). This plot demonstrates that between 19 and 21 UT the predominant location of NED echoes gradually moved from the north (near 0°) to west (-90°). At about 20 UT the NED echoes arrived from the Tromsø direction. At that time the

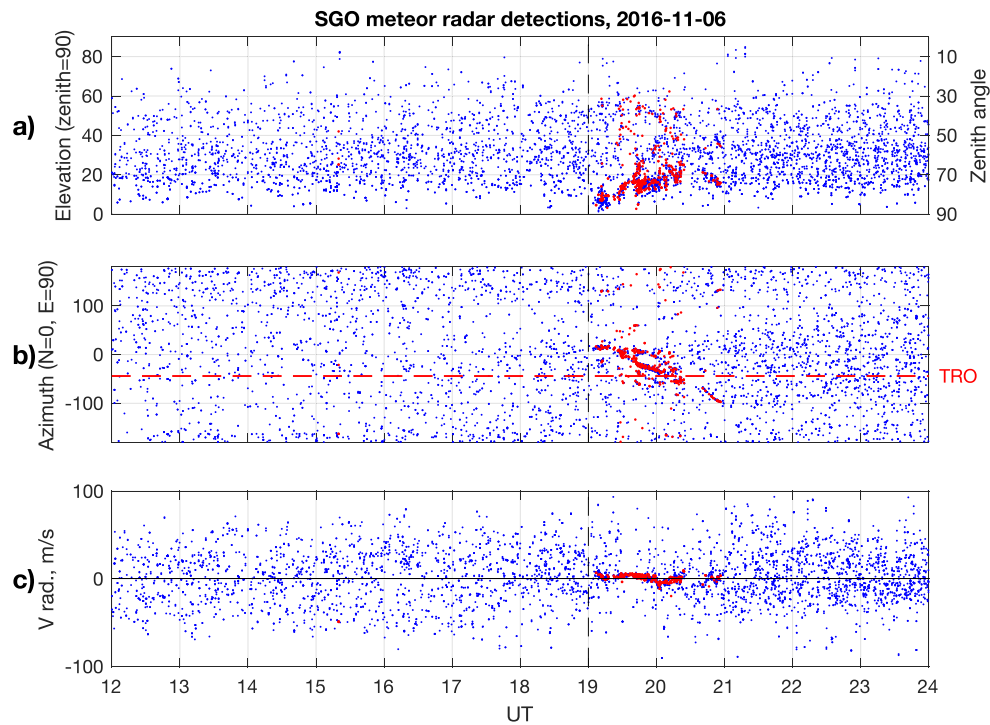


Figure 1. Parameters of the meteor radar echoes detected between 12 and 24 UT on 6 November 2016: (a) elevation; (b) azimuth, red dashed line indicates direction toward Tromsø (TRO); (c) Doppler line-of-sight velocity (+ away). Red dots indicate nonexponentially decayed echoes. SGO = Sodankylä Geophysical Observatory.

Digisonde in Tromsø detected an enhancement of the *E* layer plasma frequency of 13.9 MHz from a background level of 3 MHz, which is illustrated in Figure 4b. Figure 4c presents the ASC data as a keogram along the south-north direction. This keogram shows that between 1925 and 2025 UT an auroral arc was moving from north to south and passing over Tromsø at about 20 UT, which corresponds well to the enhancement of the *E* layer electron density and the location of the NED echoes.

Thus, we can suppose that the bending of the MR radio waves toward the ground occurred due to the high electron density in the *E* layer associated with the auroral arc. The electron density corresponding to the plasma frequency of 13.9 MHz is $2.4 \cdot 10^{12} \text{ m}^{-3}$. From the Digisonde ionogram at 20 UT, all frequencies up to 13.9 MHz were reflected from a sporadic *E* layer (*Es*) at the height of about 110 km.

The most favorable condition for obtaining ground backscatter is total internal reflection of the radio wave at the lower boundary of *Es*. According to the Snell's law, the total internal reflection occurs at incident angles greater than the critical angle θ_c , which is given by

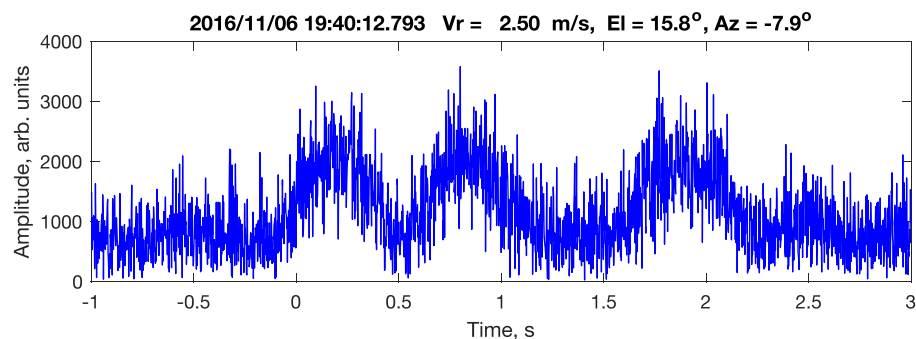


Figure 2. Amplitude of the nonexponentially decayed echo detected at 19:40:13 UT. Zero time corresponds to the time of detection.

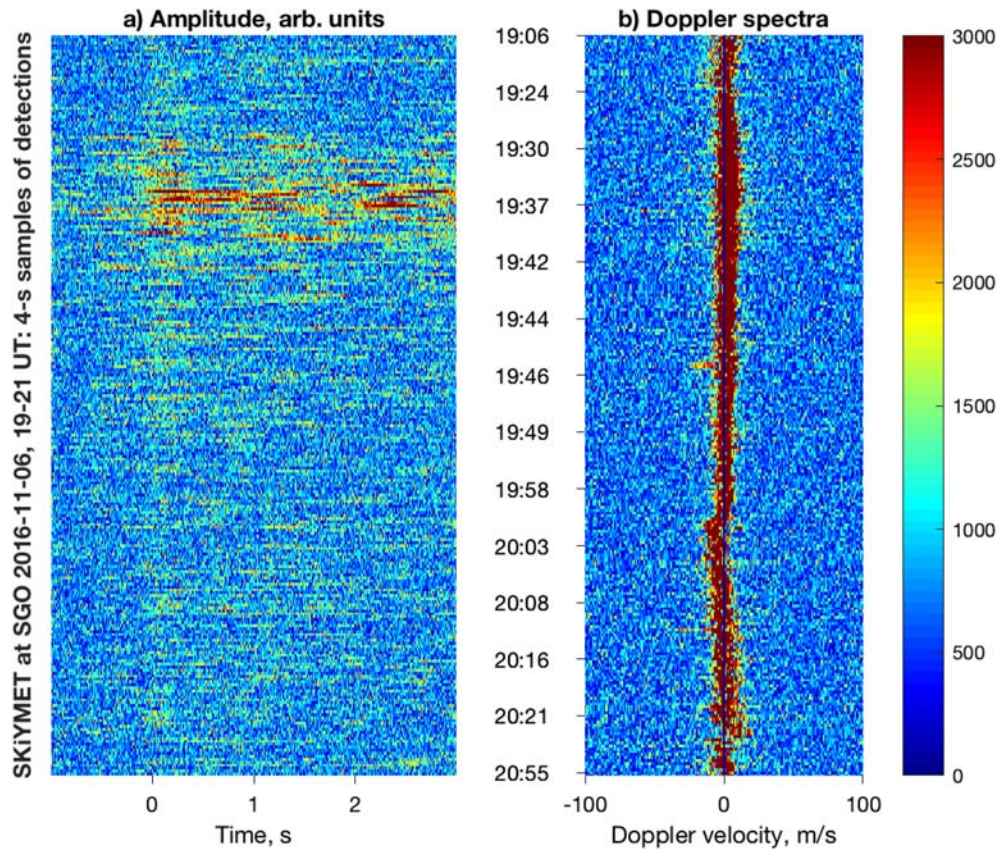


Figure 3. (a) Color-coded plot showing amplitudes of the 249 nonexponentially decayed echoes detected during the event in frame of the record duration time (horizontal axis) and time of detection (vertical axis); (b) Doppler spectra of the nonexponentially decayed echoes. The color scale on the right-hand side relates to both panels and is given in arbitrary units relevant for each panel. SGO = Sodankylä Geophysical Observatory.

$$\sin(\theta_c) = N_p = \sqrt{1 - \frac{f_p^2}{f_r^2}}, \quad (1)$$

where N_p is the refractive index of the plasma, f_p is the plasma frequency, and $f_r = 36.9$ MHz is the radar frequency. Equation (1) can be rewritten such as $f_p = f_r \cos(\theta_c)$, after which we easily obtain a minimal plasma frequency of E_s needed to reflect totally the radar wave:

$$f_{min} = f_r \cos(\theta_i), \quad (2)$$

where θ_i is an incident angle of the wave. Taking into account the curvature of the Earth, the incident angle, θ_i , is related to the elevation angle by

$$\sin(\theta_i) = \cos(el.) \frac{R_E}{R_E + h}, \quad (3)$$

where R_E is the Earth's radius and h is the height of the reflection.

The median elevation angle of the NED echoes on 6 November is 17° , with lower and upper quartiles of 14° and 22° , respectively. Assuming the height of reflection at 110 km, we obtain from (3) incident angles of 73° (for lower quartile), 70° (for median), and 66° (for upper quartile) at the points where the radio waves are incident upon the E_s layer. Corresponding minimal plasma frequencies for these angles are 11.1, 12.6, and 15.2 MHz. Such frequencies are indeed very close to the value of 13.9 MHz observed by the Tromsø Digisonde in the time of interest. This strongly supports the ground scatter hypothesis for NED echoes

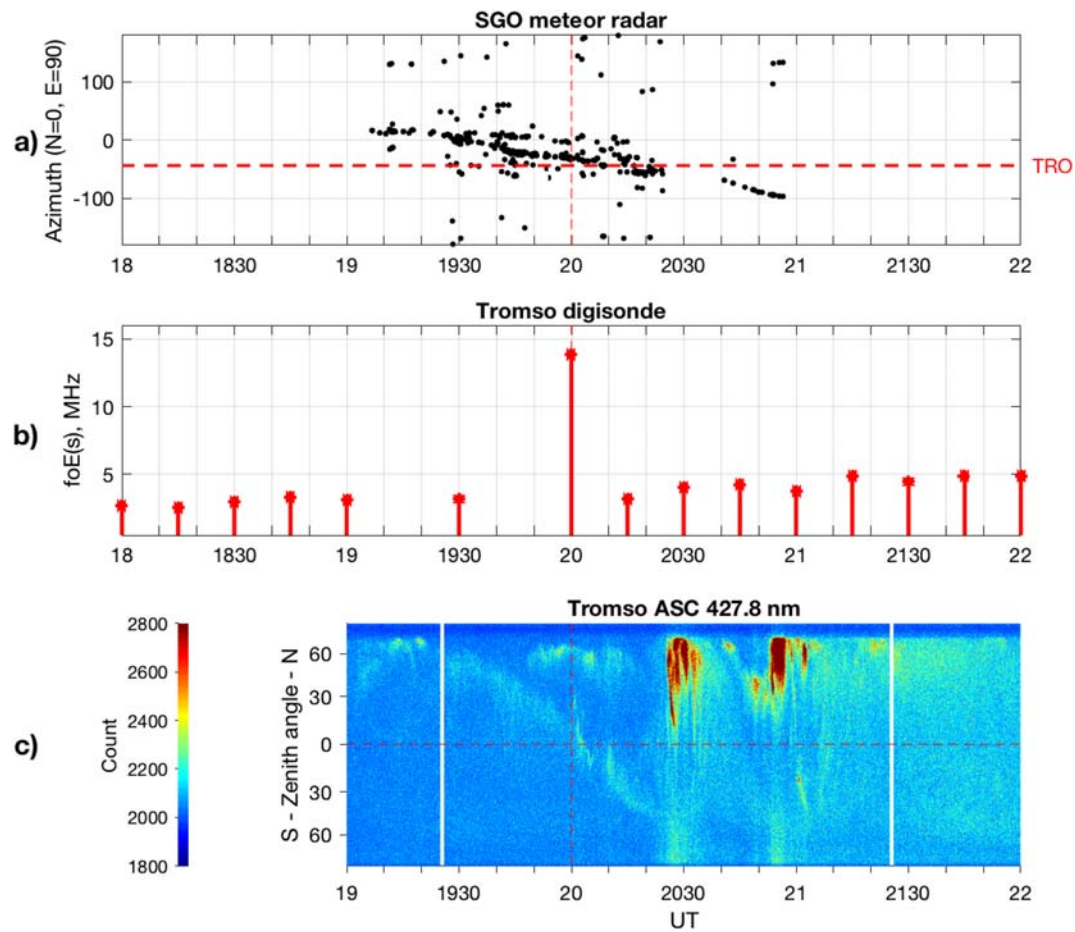


Figure 4. (a) Azimuth of the nonexponentially decayed meteor radar echoes, red dashed line indicates direction toward Tromsø (TRO); (b) maximal E layer plasma frequency measured once in 15 min by the Digisonde in Tromsø; (c) keogram of the all-sky camera (ASC) in Tromsø. SGO = Sodankylä Geophysical Observatory.

and suggests the height of mirroring at 110 km in this case. In the next section we determine the location of the mirroring and investigate how it relates to the aurora.

5. Locations of Radar Echoes and Aurora

Using the MR elevation and azimuth estimates of the targets, and assuming a height of reflection at 110 km, we have calculated the geographic positions of the NED targets. The positions are shown in Figure 5 where the color of the dots corresponds to time of the detections according to the color bar at the bottom. The reflectors were first detected at about 19 UT to the north of Sodankylä at the lowest elevation, and afterward the location of the reflector gradually moved to southwest. After 1935 UT the reflectors were detected within the field of view (FOV) of the high-speed ASC installed in Tromsø. In addition, there are some targets located around Sodankylä at higher elevation (closer to the MR zenith), although we believe that these targets were located erroneously, probably because several targets were detected simultaneously at the same gate.

In Figure 5, the solid circle around Tromsø shows the FOV of the ASC at zenith angle of 68° for a height of 110 km (its radius is 250 km). Assuming the luminosity height at 110 km (i.e., the same as the E_s height), we compare the auroral data with locations of the NED targets.

Figure 6 presents an example of such a comparison for one ASC frame. The auroral image was taken at 2017 UT, and the red dots correspond to the NED targets located during the 2 min, between 2016 and 2018 UT. This plot demonstrates a very good colocation of the NED targets and the auroral arc. Such plots were made for each minute between 19 and 20 UT, and they are given in Movie S3. As a rule, the NED targets are

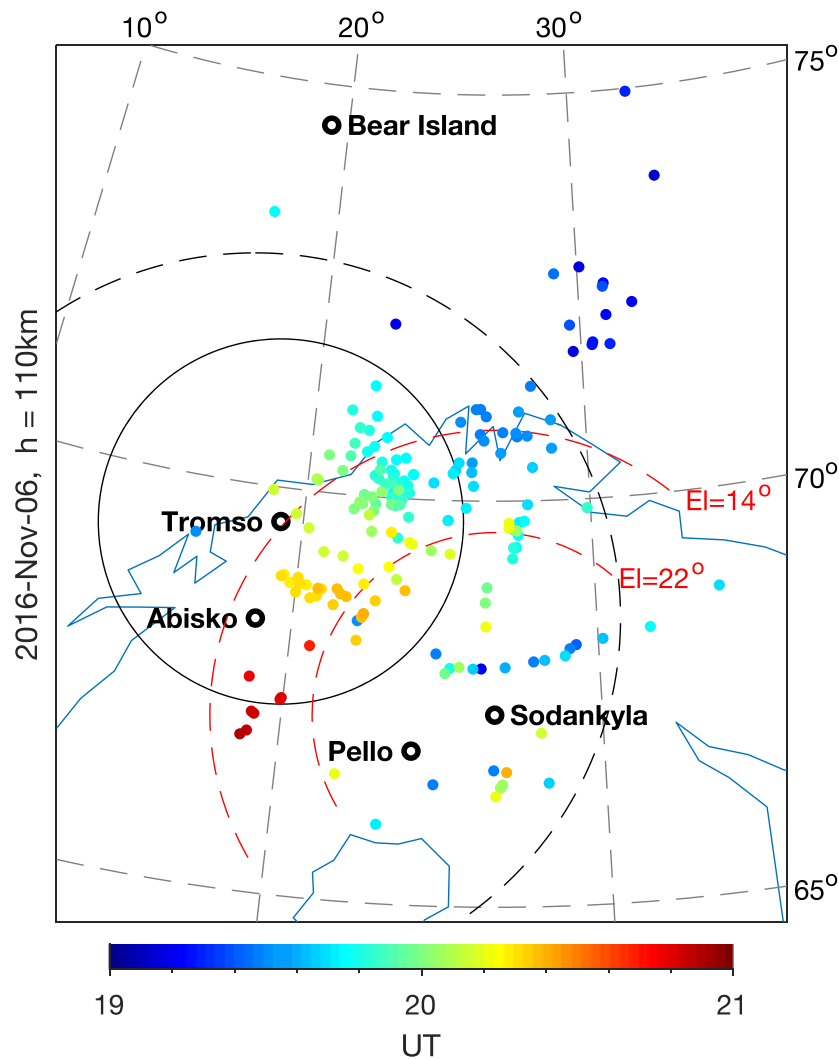


Figure 5. Geographic positions of the nonexponentially decayed (NED) targets. Color of dots corresponds to time of the detections according to the color bar in the bottom. The solid circle around Tromsø (its radius corresponds to 250 km) shows field of view of the all-sky camera at zenith angle of 68° for a height of 110 km. The dashed circle shows field of view of the all-sky camera in Abisko for the red (630 nm) emission. Red dashed circles centered at Sodankylä indicate location of meteor radar targets at elevation angles 22° and 14°, which correspond to quartiles of the distribution of NED elevations.

colocated with the auroral arc drifting toward the south, which was observed in the FOV of the ASC between 1925 and 2025 UT.

The arc was predominantly oriented east-west along a geographic latitude. For further comparison of the locations of the arc and NED targets, Figure 7 presents the ASC keogram as a function of time and geographic latitude. (Note this is different from Figure 4 where the keogram is a function of time and zenith angle). Red dots indicate the latitude of the NED targets. Taking into account the MR locations errors and possible differences in longitude, this plot clearly demonstrates colocation of the NED echoes and the auroral arc drifting to south between 1925 and 2025 UT.

During the event, the predominant azimuth of the NED targets was changing from north to west, indicating a westward drift. However, we can neither claim nor rule out that it resulted from a real westward motion of ionospheric or magnetospheric structures. Looking at Figure 5, we can see that such a motion might be solely due to the southward motion of the auroral arc. It is clear that MR ground echoes cannot be observed at large elevation angles because it would require unrealistic high ionospheric electron density. Indeed, 75% of the NED echoes were observed at an elevation lower than 22° (indicated by a dashed red circle in Figure 5),

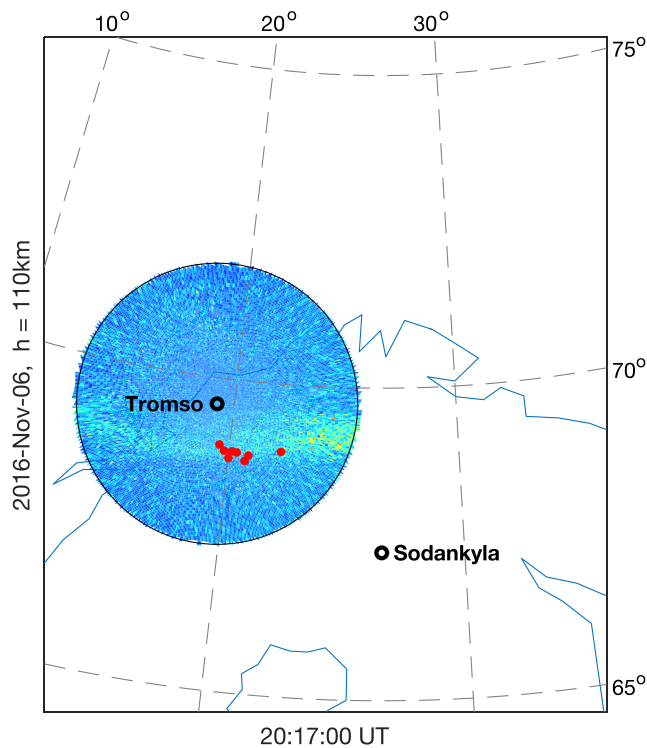


Figure 6. Comparison of the auroral data with locations of the nonexponentially decayed targets. The auroral image was taken at 2017 UT, and red dots correspond to the nonexponentially decayed targets located during 2 min, between 2016 and 2018 UT.

and most of the remaining 25% might be erroneously located at high elevation, which happens when several targets are detected simultaneously at the same gate. Thus, when the auroral arc is approaching the radar, high ionospheric electron density may be located at low elevation in the west or east. However, the sea surface that is favorable for ground scatter exists only in the west. Hence, the location of the NED echoes is moving toward the west along a circle around the radar, which may not be a real motion of the ionospheric ionization.

6. Amplitude Modulation of the Ground Echo

6.1. Auroral Fluctuations and Radar Echoes

Altogether, 89 NED echoes were received from the area within the FOV of the ASC. For all of them we investigated the correspondence of variations of the amplitude of radar return and variations of the auroral intensity. The time series were obtained with sampling rates 512 and 10 Hz, respectively. To make them comparable, the 4-s radar time series were low-pass filtered at 5 Hz and rarefied to 10-Hz sampling corresponding to the time of ASC frames.

The average height of the ionospheric reflector was estimated as 110 km, although this height might vary within a few kilometers range. At low elevation of about 17° it may lead to an error in the location of the order of 10 km. Moreover, the path of the radio waves may differ from straight lines, and there is an uncertainty in the angular location. On average, we estimate that a net uncertainty of the location may be of the order of 15–20 km.

On the other hand, the size of the pixels of the ASC frames varies from 0.2 km near zenith to 10 km at an elevation of 20°. Hence,

we cannot attribute the location of a NED target to a certain ASC pixel. To make a comparison, for each NED target within the ASC FOV we selected an area 60×60 km centered at the location of the target. Depending on the location, such an area contains from 13×13 to 56×56 pixels. In all the pixels we calculated the covariance between the ASC count and MR amplitude variations during 4 s and selected a pixel where the covariance is maximal. As an example, Figure 8 presents such an analysis for the NED

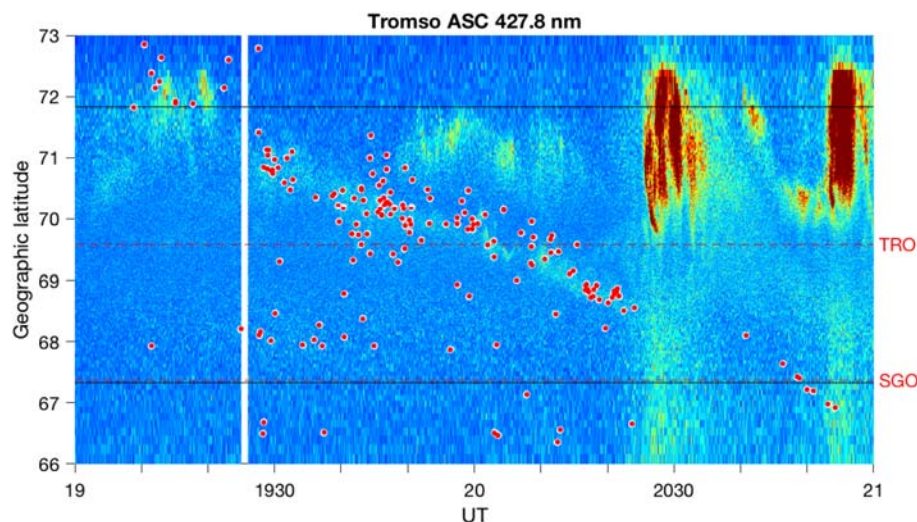


Figure 7. The Tromsø all-sky camera (ASC) keogram (same as in Figure 4c) as a function of time and geographic latitude. Red dots indicate latitude of the nonexponentially decayed targets. Dashed lines show latitudes of Tromsø (TRO) and Sodankylä (SGO). Black lines show field of view of the ASC (same as in Figure 5).

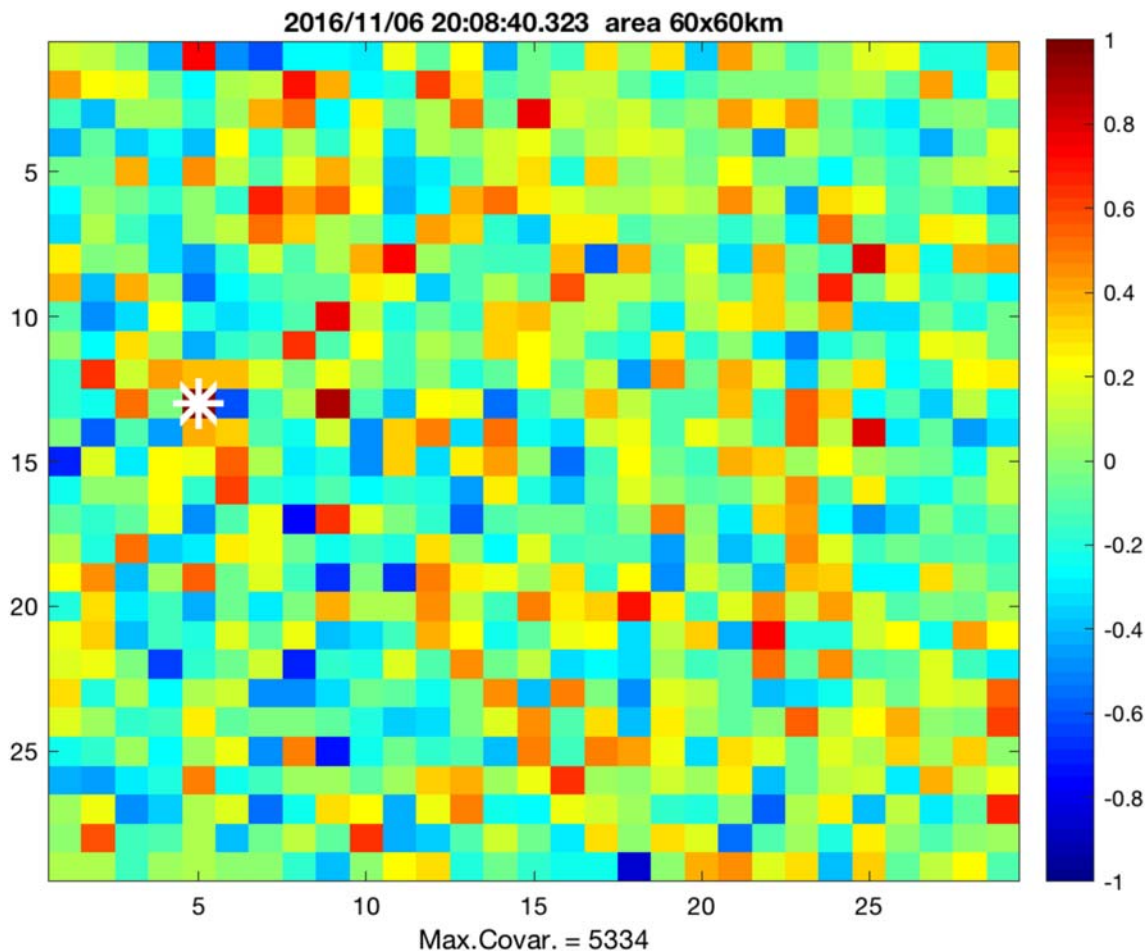


Figure 8. Covariance matrix for the nonexponentially decayed detection at 20:08:40 UT. The color plot shows values of the covariance normalized by maximum. The maximal covariance (equal to 5,334) was obtained in the pixel indicated by the white asterisk, which is at a distance of 14 km from the nonexponentially decayed location.

detection at 20:08:40 UT. The color plot shows values of the covariance normalized by the maximum. The maximal covariance (equal to 5,334) was obtained in the pixel indicated by the white asterisk. This pixel is located at a distance of 14 km from the center of the area. For this pixel Figure 9 shows comparison of the auroral (blue curve) and the MR amplitude (red curve) variations. One can see a similarity between the two curves. From the ASC pixels apart from aurora, we estimated a noise level as ± 50 counts and a background (dark) constant level as 2,000 counts. Hence, the auroral variations between 2,000 and 2,350 counts in Figure 8 exceed the noise level and may be considered as real.

In the same way as Figures 8 and 9, we made corresponding plots for all the 89 NED detections within the ASC FOV. They are presented in Supporting Information S4 and S5, respectively. Averaged over the 89 detections, the mean distance of the maximal covariance location from the center is -0.7 ± 12.2 km in the north-south direction and -0.4 ± 16.8 km in the east-west direction (see Figure S1). From Plots S4 and S5, we make two conclusions.

First, the covariance values are typically very different even in neighbor pixels. The auroral variations do not correlate at spatial scales between 1 and 5 km and look like irregular random fluctuations in the frequency range 1–5 Hz. Thus, the ionosphere is spatially and temporally irregular in the region of the auroral arc precipitation.

Second, in the vicinity of the NED targets there exists auroral activity with a temporal variability that corresponds to the amplitude variations of the radar ground scatter. Hence, such auroral precipitation might be

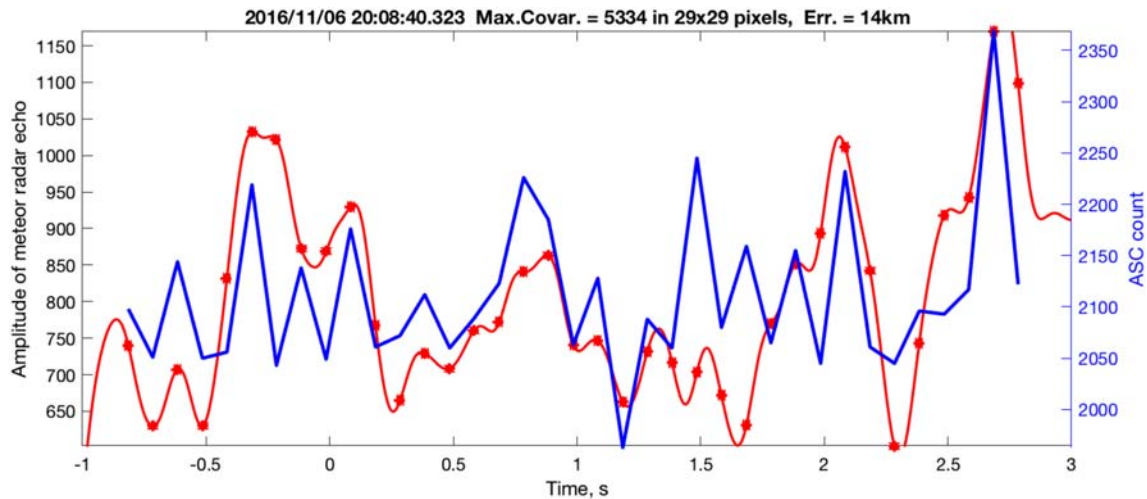


Figure 9. Comparison of the auroral (blue curve) and the meteor radar amplitude (red curve) variations for the nonexponentially decayed detection at 20:08:40 UT. ASC = all-sky camera.

responsible for the modulation of the NED echoes, although we cannot claim that reflection occurred at a certain point corresponding to a particular ASC pixel. Moreover, the waveform of the NED echoes is most probably a result of interference of the MR returns from the spatially irregular ionospheric region of the auroral arc.

6.2. Variations of the Ionospheric Electron Density

It is known that due to the ionospheric recombination time of the order of tens of seconds, few-hertz variations of auroral precipitation cannot produce noticeable enough variations in the ionospheric plasma density

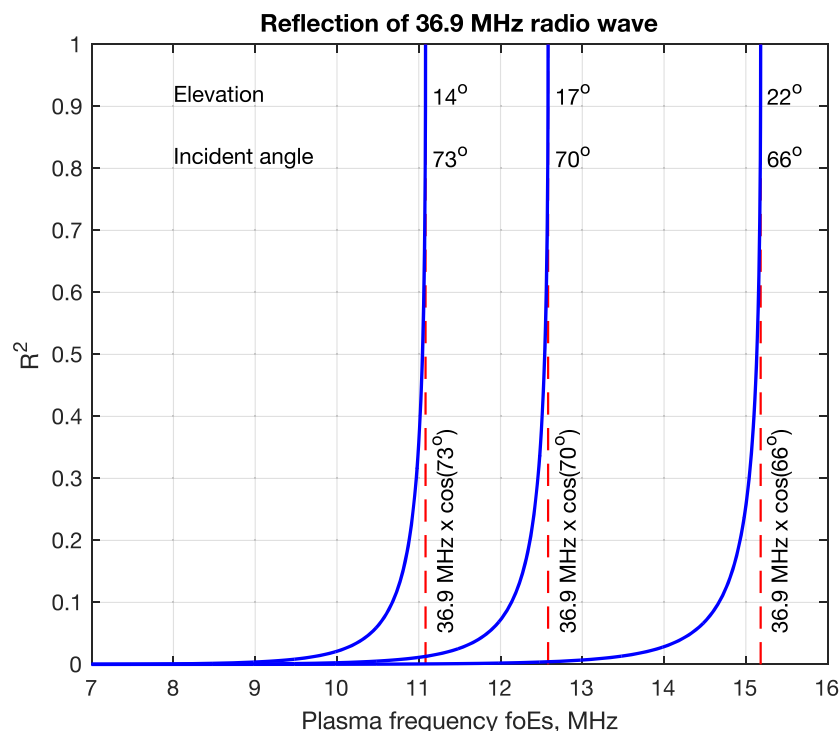


Figure 10. Reflection coefficient of meteor radar radio wave versus plasma frequency of E_s , calculated for three different elevation angles.

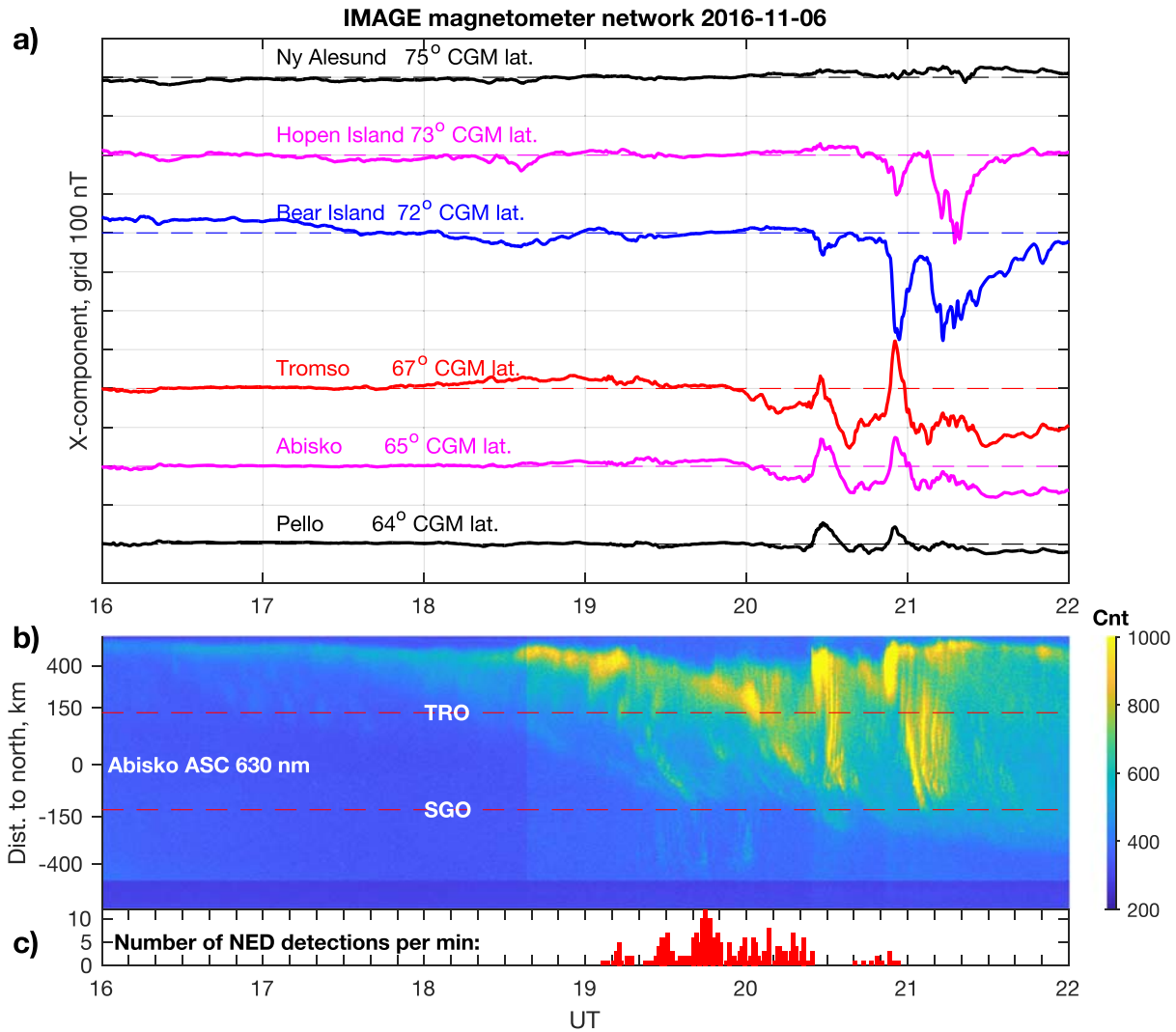


Figure 11. Geophysical conditions during the event: (a) X-component magnetograms from some observatories of the IMAGE magnetometer network; (b) keogram of the all-sky camera (ASC) in Abisko. Red dash lines on the keogram correspond to zeniths of Tromsø (TRO) and Sodankylä (SGO). (c) histogram showing a number of meteor radar nonexponentially decayed (NED) echoes detected in a minute. CGM = corrected geomagnetic; SGO = Sodankylä Geophysical Observatory.

to be detected by radars (e.g., Cosgrove et al., 2010). Nevertheless, such high-frequency variations are detected in the MR ground scatter, and below, we show why this is possible.

For a circularly polarized electromagnetic wave incident upon the lower boundary of the *Es* layer, we may calculate a reflection coefficient, that is, the fraction of the incident power that is reflected, *R*, as (e.g., Yavorskij & Detlaf, 1964)

$$R = \frac{1}{2} \left[\left(\frac{\sin(\theta_i - \theta_r)}{\sin(\theta_i + \theta_r)} \right)^2 + \left(\frac{\tan(\theta_i - \theta_r)}{\tan(\theta_i + \theta_r)} \right)^2 \right], \quad (4)$$

where

$$\sin(\theta_r) = \sin(\theta_i)/N_p \quad (5)$$

and θ_r is a refraction angle.

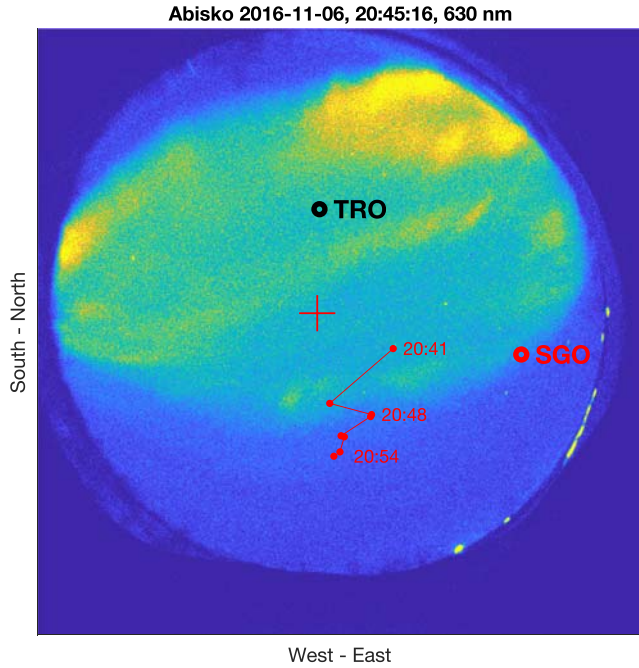


Figure 12. A frame of the Abisko all-sky camera at 2045 UT. Position of Sodankylä Geophysical Observatory (SGO) is indicated by a red circle. Locations of the nonexponentially decayed echoes detected between 2041 and 2054 UT are shown by red dots, and the red broken line connects locations of subsequent echoes.

Since the signal received as ground scatter passes through the ionosphere twice, that is, there are two reflections along the whole path, the fraction of the returned power is R squared. This value calculated for three different elevation angles is presented in Figure 10 versus plasma frequency of E_s ($foEs$). The angles correspond to the median elevation angle of the NED echoes on 6 November (17°) and lower and upper quartiles (14° and 22° , respectively), which were discussed in section 4. Once again this plot shows the critical plasma frequencies (11.1, 12.6, and 15.2 MHz), which are required for total internal reflection of the MR waves. The other important feature illustrated in the plot is that near the critical frequencies even small variations in the $foEs$ (about 0.5%) cause large variations of the power of return (by more than 50%). Hence, even small changes of the E layer electron density (less than 1%) may cause noticeable modulation of the radar return. In the following we estimate whether auroral pulsations at a frequency of 2 Hz can produce such changes in the ionosphere.

We use the continuity equation for E region electron density where the transport term is neglected:

$$\frac{\partial n}{\partial t} = Q - \alpha n^2. \quad (6)$$

The production term consists of a constant and oscillating parts:

$$Q = Q_0(1 + \gamma e^{-i\omega t}), \quad (7)$$

where $0 \leq \gamma \leq 1$. The electron density is the sum of the background and oscillating parts:

$$n = n_0 + \delta n e^{-i\omega t}. \quad (8)$$

After linearization (6) by taking into account $|\delta n| \ll n_0$, we obtain

$$\frac{|\delta n|}{n_0} = \gamma \frac{\alpha n_0}{\omega}. \quad (9)$$

For the electron density $2 \cdot 10^{12} \text{ m}^{-3}$ corresponding to a plasma frequency of 13 MHz and $\alpha n_0 = 0.2 \text{ s}^{-1}$, about 1% modulation of the electron density at 2 Hz ($\omega = 12.6 \text{ s}^{-1}$) may be obtained, which causes about 50% modulation of the power of MR ground echo.

Thus, we see that a dense sporadic E layer is the most important condition for obtaining MR NED echoes. First, a high $foEs$ is required for reflection of the 36.9-MHz radio wave toward the ground and obtaining the ground scatter. Second, to be accepted as a meteor echo, a high-frequency (about 2 Hz) amplitude modulation of the received signal is needed, and from (9) one can see that a high enough electron density in the E_s layer is the most important condition for obtaining a noticeable modulation of the amplitude of the radar return. From the above consideration, it follows that the MR interprets a ground scatter as a meteor echoes if

$$f_o E_s = f_r \cos(\theta_i) \approx f_r \sin(el.). \quad (10)$$

Hence, NED MR echoes may be used for estimating the E layer electron density.

Initially, Kozlovsky and Lester (2015) proposed that precipitation associated with pulsating aurora might be responsible for modulation of the ionospheric electron density. After the above consideration, we can conclude that the modulation may be caused by random irregular fluctuations of auroral precipitation, although we do not rule out possible role of more regular auroral oscillations to produce NED echoes such as, for example, that shown in Figure 2.

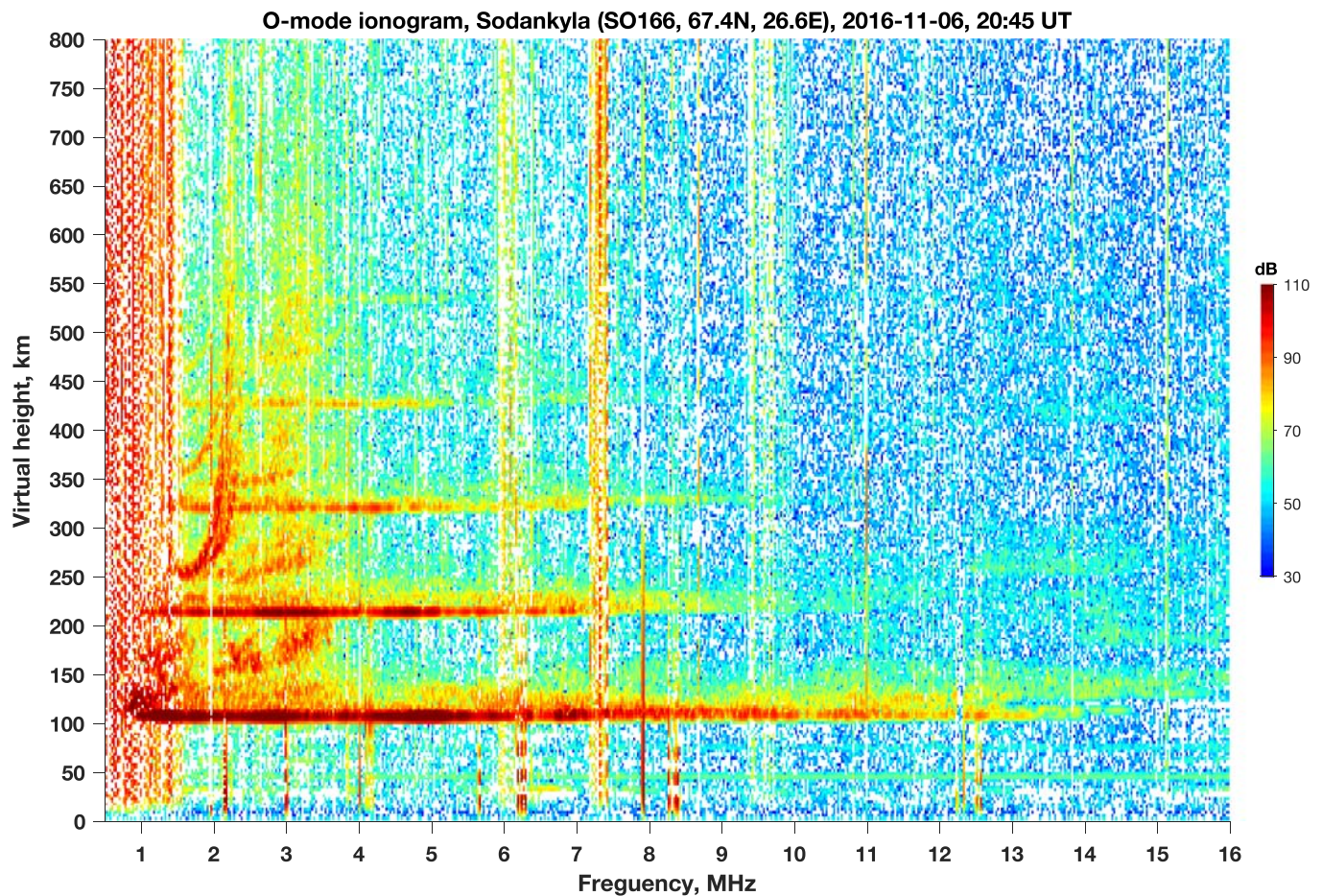


Figure 13. The Sodankylä Geophysical Observatory ionogram showing a dense multiple *Es* at 20:45 UT.

Obviously, for lower elevation angles a smaller *Es* electron density is required for achieving the ground scatter. On the other hand, lower elevation corresponds to a larger distance to the reflection point, such that the amplitude of NED should be small. Indeed, a few NED echoes were obtained at low elevation, but they were obtained from the same region at about the same time (dark blue dots in Figure 5). This allows us to suppose that this was not an error and the distant propagation was real.

Statistical analysis (see Figure S2) has shown that majority of the NED echoes were obtained from the bending points between 200 and 450 km, which may correspond to the distances to ground reflectors from 400 to 900 km. Within this range, amplitudes of the detections were between 1,000 and 2,500 arbitrary units, and no any dependence on the distance was found. Perhaps it was because of highly variable ionospheric conditions.

7. Geophysical Conditions

7.1. The Substorm Growth Phase

Figure 11 shows the geophysical conditions during the event. Figure 11a presents X- component magnetograms from some observatories of the IMAGE magnetometer network, the positions of which are indicated in the map in Figure 5. Figure 11b shows keogram of the ASC in Abisko (see map in Figure 5). The keogram is made from red filter images (630 nm) taken at a rate of 2 frames per minute. Red dash lines on the keogram correspond to zeniths of Tromsø and Sodankylä. The height of the red emission is assumed at 200 km (Jackel et al., 2003). A histogram in Figure 11c shows number of MR NED echoes detected in a minute.

The majority of the NED echoes were observed between 1906 and 2024 UT, which was in the substorm growth phase when a quiet prebreakup auroral arc was drifting from north to south in the FOV of the

ASC. At about 2000 UT the arc was located near zenith of Tromsø. At that time, the Digisonde in Tromsø detected the dense sporadic *E* layer.

At 2024 UT an auroral intensification occurred to the north of Tromsø, which is seen in the keograms and also indicated in the magnetic field data. During the intensification, the auroral oval sharply expanded to the south and reached the latitude of SGO at about 2030 UT. During the auroral intensification at 2025–2040 UT, no NED echoes were detected. After that, at 2040–2055 UT, some NED echoes were observed until the substorm breakup, which occurred poleward of Tromsø.

Kozlovsky and Lester (2015) found that NED echoes are typically associated with substorms, although they did not specify phases of the substorm. They provided a list of 73 NED events during 2009–2014. We checked carefully IMAGE magnetometer network data for these cases and found that the majority of the events occurred in the substorm growth phase, and subsequent breakups occurred at higher latitudes (poleward of 67° CGM latitude), similar to the present case. At the moment of breakup, the detection of NED echoes stopped. This agrees with the result of the present case study. We may assume that favorable conditions for the dense *Es*, which is necessary for NED echoes, tend to appear during the substorm growth phase and are associated with prebreakup auroral arcs. More active aurora during the breakup may be associated with enhanced ionization in *D* layer and, hence, absorption of the radio waves scattered from ground. However, for a solid conclusion, more cases of auroral observations associated with NED echoes are to be studied in future.

7.2. Sporadic Auroral E Layer in the SGO Ionosonde Data

Figure 7 shows that between 2041 and 2054 UT, NED echoes were detected at the latitude of Sodankylä. Because of the large distance or maybe clouds, the ASC in Tromsø was not able to observe aurora there. However, at this time the ASC in Abisko (at 630 nm) observed a southward moving aurora at the latitude of SGO (Figure 11b).

Figure 12 presents a frame of the Abisko ASC at 2045 UT when the auroral arc was observed over SGO, the position which is indicated by a red circle on the frame. For calculating positions on the frame, a mapping between heights of 110 and 200 km was made with taking into account the magnetic field inclination of 78°. Locations of the NED echoes detected between 2041 and 2054 UT are shown by red dots, and the red broken line connects locations of subsequent echoes. The location of NED targets moved toward the south following the southward drift of the auroral arc. Thus, at about 2045 UT the SGO ionosonde was able to observe the same auroral arc, which was responsible for the MR NED echoes (although bending of the MR radio waves occurred some 300 km away from the point of the ionosonde sounding).

The SGO ionogram presented in Figure 13 was obtained at 2045 UT when the arc was above Sodankylä. The ionogram shows a dense *Es* ($f_oE_s \approx 13$ MHz) at a height of about 110 km. Multiple (up to five) *Es* traces indicate good reflectivity of the layer. A sharp *Es* trace at frequencies up to about 13 MHz indicates a sharp lower edge of the dense layer, which reflected radio waves like a mirror. These data give additional support to the conclusions of the study.

According to Rees (1963), to produce such ionization at 110 km, the energy of precipitating electrons must be about 5 keV. The multiple *Es* traces indicate also low absorption; hence, higher energy electron precipitation (tens of keV) is not essential at this place. This agrees with the result of Kirkwood and Eliasson (1990) who found that (citation) “Southward drifting auroral arcs which also characterize the substorm growth phase are found to be located immediately poleward of the zone of higher-energy electron precipitation, i.e., immediately poleward of the stable trapping boundary for > 10 -keV electrons.” Spatial separation between the growth phase arc and the region of cosmic noise absorption (caused by precipitation of > 10 -keV electrons) is of the order of 40 km (McKay et al., 2018).

8. Summary

Multi-instrument observations using a MR, auroral cameras, ionosondes, and ground magnetometers were made in Northern Europe at auroral latitudes (between 64° and 72° CGM latitude) at 22–24 magnetic local time during a substorm growth phase. The southward drifting growth phase auroral arc was associated with enhanced electron density up to $2 \cdot 10^{12} \text{ m}^{-3}$, corresponding to about 13-MHz plasma frequency, f_oE_s , at an

altitude of about 110 km. Such enhanced E layer ionization caused bending toward ground of the 36.9-MHz MR radio waves transmitted at low ($<25^\circ$) elevation, such that the radar received ground echoes characterized by a near-zero Doppler shift. The amplitude of the echoes was modulated at a frequency of a few hertz, and similar modulation was found in the auroral luminosity at 427.8 nm near the locations of the bending of MR radio waves. In the given case the modulation was due to irregular (random) fluctuations of auroral precipitation.

It has been shown that such a few-hertz variations of the auroral precipitation cannot produce more than 1% modulation of the ionospheric electron density, although even such small modulation can lead to 50% modulation of the MR ground scatter if $f_oE_s \approx f_r \sin(\epsilon_l)$. The ionosonde and MR data provide evidence that this condition was satisfied in the present case.

Due to a high-frequency (>2 Hz) amplitude modulation of the ground scatter, the MR erroneously accepts such signals (referred as NED echoes) as echoes from meteor trails. We have shown that a dense auroral sporadic E layer is the most important condition for obtaining MR NED echoes. First, a high f_oE_s is required for reflection the 36.9-MHz radio wave toward the ground and obtaining the ground scatter. Second, to be accepted as a meteor echo, a high-frequency (about 2 Hz) amplitude modulation of the received signal is needed, and from (9) one can see that high enough electron density in the auroral E_s layer is the most important condition for obtaining a noticeable modulation of the amplitude of the radar return. Thus, in some cases the MR may be used for estimating the E layer electron density.

Finally, we mention one further important condition for obtaining the ground scatter is presence of certain scale sea waves, which are necessary for Bragg backscatter of the MR radio waves. Hence, weather and ice conditions in the Arctic Ocean may essentially affect the occurrence of the NED echoes.

Acknowledgments

The data of the meteor radar, SGO ionosonde, and Abisko ASC were collected at SGO (<http://www.sgo.fi/>). The operation of the EMCCD camera at Tromsø has been supported by JSPS KAKENHI JP 15H05747 and the Arctic University of Norway (UiT). The data files are obtained from ERG-Science Center operated by ISAS/JAXA and ISEE/Nagoya University (at https://ergsc.isee.nagoya-u.ac.jp/data_info/ground.shtml.en). Data of the Digisonde were obtained from the Tromsø Geophysical Observatory of the Arctic University of Norway (<http://geo.phys.uit.no/ionodata/index.html>). Data of the IMAGE magnetometer network are available online (at <http://space.fmi.fi/image/www/>). We thank the institutes who maintain the IMAGE Magnetometer Array: Tromsø Geophysical Observatory of UiT the Arctic University of Norway (Norway), Finnish Meteorological Institute (Finland), Institute of Geophysics Polish Academy of Sciences (Poland), GFZ German Research Centre for Geosciences (Germany), Geological Survey of Sweden (Sweden), Swedish Institute of Space Physics (Sweden), Sodankylä Geophysical Observatory of the University of Oulu (Finland), and Polar Geophysical Institute (Russia). S. S. acknowledges support from the Academy of Finland via Grant 310348. M. L. acknowledges support from STFC Grants ST/S000429/1 and ST/N000749/1. A. K. acknowledges discussions within the International Space Science Institute (ISSI) Team 410 on New Features in the Meteor Radar Observations and Applications for Space Research.

References

- Cosgrove, R., Nicolls, M., Dahlgren, H., Ranjan, S., Sanchez, E., & Doe, R. (2010). Radar detection of a localized 1.4 Hz pulsation in auroral plasma, simultaneous with pulsating optical emissions, during a substorm. *Annales de Geophysique*, 28, 1961–1979. <https://doi.org/10.5194/angeo-28-1961-2010>
- Enell, C.-F., Kozlovsky, A., Turunen, T., Ulich, T., Väitalo, S., Scotto, C., & Pezzopane, M. (2016). Comparison between manual scaling and Autoscala automatic scaling applied to Sodankylä Geophysical Observatory ionograms. *Geoscientific Instrumentation, Methods and Data Systems*, 5, 53–64. <https://doi.org/10.5194/gi-5-53-2016>
- Hall, C., & Hansen, T. L. (2003). 20th Century operation of the Tromsø Ionosonde. In: *Advances in Polar Upper Atmosphere Research 2003* (17). ISSN 1345-1065, 155–166.
- Hocking, W. K., Fuller, B., & Vandepere, B. (2001). Real-time determination of meteor-related parameters utilizing modern digital technology. *Journal of Atmospheric and Solar - Terrestrial Physics*, 63, 155–169.
- Jackel, B. J., Creutzberg, F., Donovan, E. F., & Cogger, L. L. (2003). Triangulation of auroral red-line emission heights. In K. U. Kaila, J. R. T. Jussila, & H. Holma (Eds.), *Proceedings of the 28th Annual European Meeting on Atmospheric Studies by Optical Methods*, (Vol. 92, pp. 97–100). Oulu, Finland: Sodankylä Geophysical Observatory Publications.
- Kirkwood, S., & Eliasson, L. (1990). Energetic particle precipitation in the substorm growth phase measured by EISCAT and Viking. *Journal of Geophysical Research*, 95, 6025–6037.
- Kozlovsky, A., & Lester, M. (2015). On the VHF radar echoes in the region of midnight aurora: Signs of ground echoes modulated by the ionosphere. *Journal of Geophysical Research: Space Physics*, 120, 2099–2109. <https://doi.org/10.1002/2014JA020715>
- McKay, D., Partamies, N., & Vierinen, J. (2018). Pulsating aurora and cosmic noise absorption associated with growth-phase arcs. *Annales de Geophysique*, 36(59–69), 2018. <https://doi.org/10.5194/angeo-36-59-2018>
- Miyoshi, Y., Shinohara, I., Takashima, T., Asamura, K., Higashio, N., Mitani, T., et al. (2018). Geospace Exploration Project ERG. *Earth, Planets and Space*, 70(1). <https://doi.org/10.1186/s40623-018-0862-0>
- Rees, M. H. (1963). Auroral ionization and excitation by incident energetic electrons. *Planetary and Space Science*, 11, 1209–1218.
- Samson, J. C., Greenwald, R. A., Ruohoniemi, J. M., & Baker, K. B. (1989). High-frequency radar observations of atmospheric gravity waves in the high-latitude ionosphere. *Geophysical Research Letters*, 16, 875–878. <https://doi.org/10.1029/GL016i008p00875>
- Samson, J. C., Greenwald, R. A., Ruohoniemi, J. M., Frey, A., & Baker, K. B. (1990). Goose Bay radar observations of Earth-reflected, atmospheric gravity waves in the high-latitude ionosphere. *Journal of Geophysical Research*, 95(A6), 7693–7709. <https://doi.org/10.1029/JA095iA06p07693>
- Tanskanen, E. I. (2009). A comprehensive high-throughput analysis of substorms observed by IMAGE magnetometer network: Years 1993–2003 examined. *Journal of Geophysical Research*, 114, A05204. <https://doi.org/10.1029/2008JA013682>
- Yavorskij, B. M., & Detlaf, A. A. (1964). *Spravochnik po fizike*, (p. 848). Moscow, Russia: Nauka.